Fermi National Accelerator Laboratory
Scuola Normale Superiore
University of Pisa
Northwestern University

Fermilab Summer Students 2016

A measurement and a simulation of the gamma background at the NEXUS@FNAL facility

Tommaso Pajero

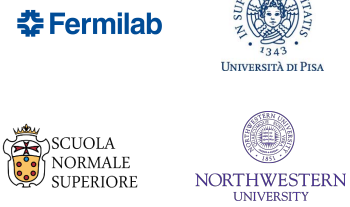

supervised by
Dr. Ziqing Hong

September 24, 2016

Contents

Acknowledgements

I wish to express my sincere thanks to Ziqing Hong for the patience and helpfulness that he demonstrated supervising my project this summer. It was my first time working in a direct detection experiment for the the search of dark matter and using *Geant4* and this work wouldn't have been possible without his careful assistance. I am also grateful to Lauren Hsu for her valuable advice about the data acquisition system and the interpretation of the data that I took at the laboratory. Last but not least, Enectali Figueroa-Feliciano greatly helped me to organize the whole project and answered with patience and competence all my not always intelligent questions about NEXUS@FNAL facility and SuperCDMS experiment.

Finally, I would like to thank all the organizers of the Summer Students project and the members of CAIF - in particular Emanuela Barzi, Giorgio Bellettini and Simone Donati - for having given me the possibility to have this wonderful experience at Fermilab.

Chapter 1

Introduction

The determination of the nature of dark matter (DM) is one of the main open problems currently faced by particle and astroparticle physics. Although the existence of DM is well established both at galactic and at cosmological scale [1] and there is compelling evidence that it constitutes about 27% of the energy content of the universe [2], both its mass and the strength of its interactions with Standard Model particles are still unknown.[1] One well theoretically motivated possibility is that DM consists of weakly interacting massive particles (WIMPs) [4], such as the lightest stable particle in supersymmetric models.

1.1 SuperCDMS experiment and iZIP detectors

According to astrophysical observations the earth is surrounded by a halo of DM with a density of about 0.4 $\text{GeV}/\text{cm}^3/c^2$. Direct detection experiments are a broad class of experiments aimed at measuring the recoils of the nuclei caused by elastic scattering with a WIMP in the active target material of a detector [5]. The detector technologies and target materials change from experiment to experiment but all these searches share the need of an extremely low background operation - because the nuclei interaction with the WIMPs, if any, is expected to be very small - and a sensitivity to recoil energies typically in the range $1 \sim 200$ keV for WIMP masses in the range $10\ \text{GeV}/c^2 \sim 100\ \text{TeV}/c^2$.

SuperCDMS is a direct detection experiment which employs germanium and silicon crystals operated at mK temperature as active detectors [6].[2] Its upgrade, which shares the same name, will be located in the SNOLAB underground laboratories in Canada and is scheduled to start to take data in 2020 with upgraded low-radioactivity setup, cryogenics and detectors. The detector module is called iZIP (interleaved Z-dependent Ionization and Phonon) and is organized in stacks of three to six detectors, which together with the copper case and the readout form a "SuperCDMS tower". It consists of a cylindrical crystal of diameter 100 mm and height 33.3 mm and is instrumented on its flat faces with interleaved ionization and phonon sensors. The simultaneous measurement of the ionization and of the phonon energy released in the recoils in the crystal allows to reject the main backgrounds of the experiment. From these measurements, in fact, it is possible to reconstruct the total recoil energy and it turns out that the ionization yield, i.e. the ratio of the ionization energy to the total recoil energy, is much lower for nuclear recoils (similar to WIMP events) than for electron recoils caused by background electrons and/or photons colliding with an atomic electron (Fig. 1.1).[3] Taking advantage of this fact, together with other more sophisticated cuts, it is possible to obtain a rejection power better than 10^6 for the background events,[4] whereas maintaining about 95% of the signal due to the WIMPs.[5]

[1] For details, recent reviews and further references about particle DM and Beyond Standard Model theories see [3].

[2] For a clear explanation of the principles of operation of the experiment see the article from one of its previous versions, CDMSII [7].

[3] The ionization yield is usually normalized so that it is equal to unity for electron recoils.

[4] The rejection power is defined as the reciprocal of the fraction of background events which survive the cuts.

[5] Some of the cuts, for example, reject surface events for which the ionization efficiency is lower than for bulk events.

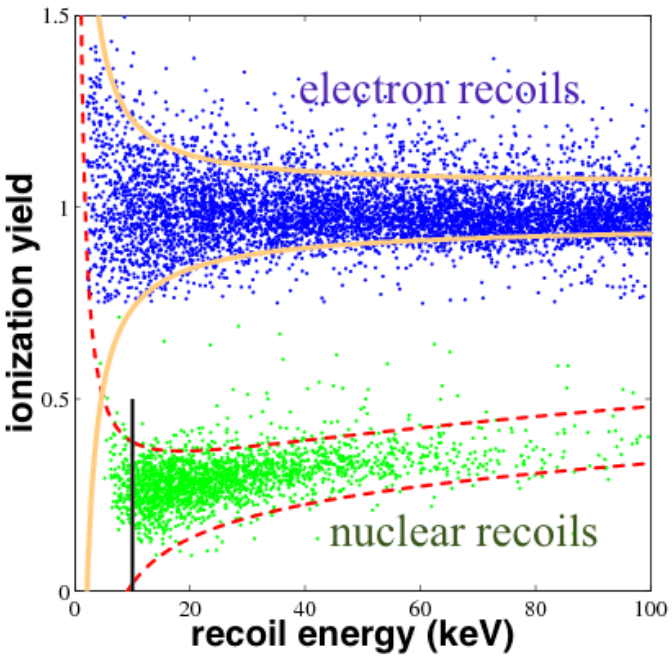

Figure 1.1: Particle identification with iZIP detectors: the ionization yield is quenched for neutron (and WIMPs) events with respect to electron and gamma scattering events (figure taken from [8]).

1.2 SuperCDMS HV detectors

The sensitivity of iZIP detectors to the low energy recoils events ($m_{WIMP} < 10$ GeV/c^2) is limited by the readout noise for both the phonon and the ionization measurement;[6] moreover, the smaller the WIMP mass, the worse the particle identification. One possible solution to overcome this problem is to renounce to the particle identification in favour of a better energy resolution. This can be achieved by applying a strong drift electric field to the crystal ($\sim$ 30 V/cm). The electron-hole pairs that are created in the ionization process are thus accelerated and the energy that they acquire during the drift (i.e. NeV_b where N is the number of the electron-hole pairs, e is the electron charge and V_b the bias voltage) is nearly entirely converted into phonons by Neganov-Luke effect (Fig. 1.2) [9]. It turns out that at this high electric field the primary phonons produced in the recoil are negligible and the phonon energy is proportional to the initial number of electron-hole pairs. The amplification of the ionization signal allows to measure the number of electron-hole pairs down to a few. Thus, if the relationship between the recoil energy and the ionization energy is known, it is possible to measure energy recoils down to 100 eV. The con of this approach is that the information of the primary phonons energy is lost and therefore the particle identification and the electron recoils background subtraction are no longer possible.

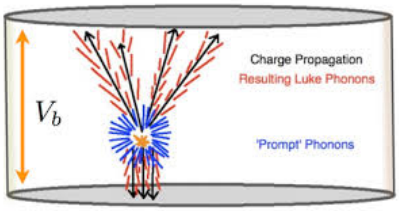

Figure 1.2: Scheme of operation of a SuperCDMS HV detector.

The aforementioned solution is adopted by the SuperCDMS HV experiment (already known as CDMSlite) [10], which set the most precise upper limits to date on spin independent cross sections for WIMP masses between 1.6 GeV/c^2 and 5.5 GeV/c^2. The upgrade of the experiment, expected to start its data taking in 2020, would improve the upper limits for masses between 1 GeV/c^2 and 10 GeV/c^2 up to five orders of magnitude (Fig. 1.3).

[6] The recoil energy is directly proportional to the square of the DM mass for masses smaller than the target one.

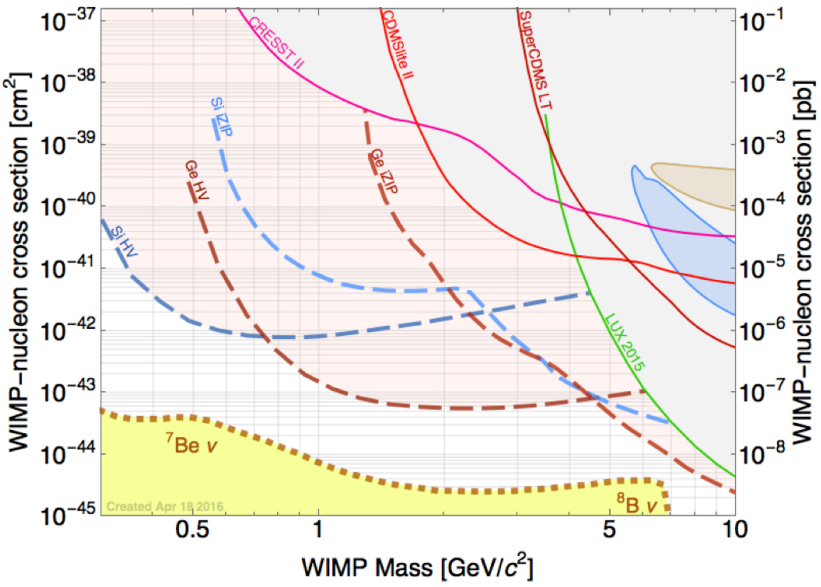

Figure 1.3: Projected exclusion plot for the SuperCDMS and SuperCDMS HV experiment (figure taken from [11]). Solid lines represent current state-of-art exclusion limits from direct detection experiments; the projected sensitivities are plot with dashed lines and are calculated using the *optimum interval method* [12] and supposing a data taking of 5 years with 80% duty cycle.

1.3 Calibration of the detectors

A better determination of the relationship between the ionization energy and the recoil energy for neutron recoils is one of the most important calibrations needed for the upgrade of the SuperCDMS HV experiment. The detection of WIMPs signal for WIMP masses in the range $1 \sim 10$ GeV/c^2 requires the measurement of recoil energies down to 100 eV. To date, only few experimental points are available under 1 keV and no one under 250 eV for germanium and Lindhard theoretical model [13], which is usually used to extrapolate the behaviour of the ionization energy at low recoil energies, has been shown to be in strong tension with the experimental data already at the keV scale for silicon [14] (Fig. 1.4). Moreover, the relationship depends slightly also on the crystal purity and drift electric field of the specific detector. Therefore, it is essential to perform a new calibration of the ionization energy, preferably with the same detectors which will be eventually employed in the actual experiment.

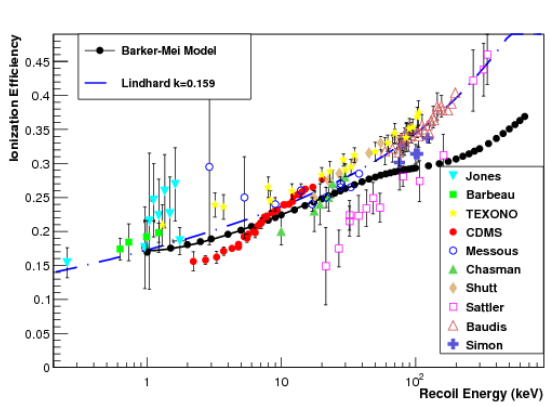

(a) Germanium crystals (figure taken from [15]); the ionization yield is defined as the ratio of the ionization energy over the recoil energy.

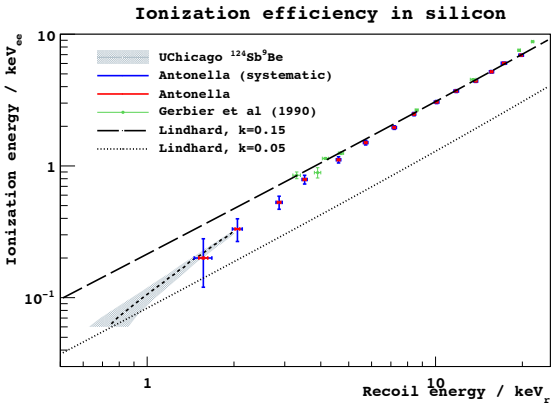

(b) Silicon crystals (figure taken from [16]).

Figure 1.4: Measurement of the relationship between the ionization energy and neutron recoil energy for germanium and silicon crystals.

This calibration of the phonon energy measured in SuperCDMS HV detectors[7] as a function of the recoil energy can be performed using the experimental apparatus in Fig. 1.5. A monochromatic beam of neutrons is aimed at a SuperCDMS detector and a fraction of them scatters elastically on its target material (Si or Ge); their scattering angle is measured with a fine-grained neutron detectors array. The energy transferred from the neutrons to the target material can then be calculated from kinematics:

$$\Delta E = 2E_n \frac{M_n^2}{(M_n + M_T)^2} \left(\frac{M_T}{M_n} + \sin^2\theta - \cos\theta \cdot \sqrt{\left(\frac{M_T}{M_n}\right)^2 - \sin^2\theta} \right)$$

where E_n is the initial neutron energy, M_n and M_T are the neutron and the target atom mass respectively and θ is the neutron scattering angle. The desired calibration can then be accomplished by comparing the calculated recoil energy with the energy directly measured by the detector.

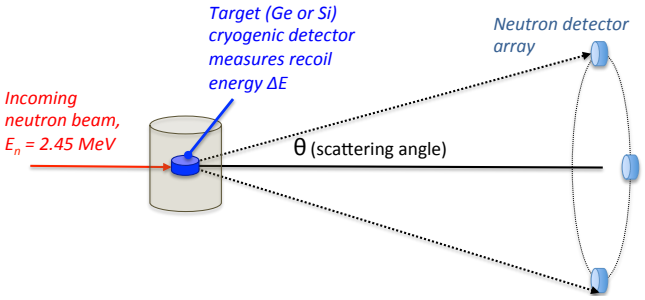

Figure 1.5: Scheme of the apparatus to perform the energy calibration of the SuperCDMS HV detectors.

Such a calibration can't, however, be adequately performed in surface neutron facilities because the dead time for SuperCDMS HV detectors is about 50 ms and the background from cosmic rays would saturate the detectors reading capability. An underground, low-background facility provided with a monochromatic neutron source is therefore required to carry out the calibration of the detectors.

1.4 NEXUS@FNAL facility

NEXUS@FNAL (Northwestern EXperimental Underground Site at Fermilab) will be a low-background underground testing facility. It will be located in the NuMI access tunnel next to the MINOS cavern, with an overburden of about 300 m water equivalent for cosmic muons which attenuates their flux to about 0.5 $m^{-2}s^{-1}$ and efficiently stops all hadronic showers from cosmic rays. That means that the expected dominant background will be that from radiogenic decays in the walls of the cavern and in the experimental apparatus itself.

The facility, which will be contained in a clean room, will be provided with a dry dilution cryogenic fridge with base operating temperature under 20 mK to allow the calibration and testing of the cryogenic detectors; a deuteron-deuteron neutron generator with a collimator will provide 2.45 MeV neutrons with an energy spread of a few percent.[8] Therefore, it is expected that the main error of the measurement of the nuclear recoils in the detector target will be that on the scattering angle due to the granularity of the neutron detector array.

The radiogenic background of neutrons and gamma rays from the cavern walls will be lowered by putting a square bucket consisting of a 10 cm lead shielding surrounded by 20 cm of plastic neutron moderator around the fridge. This shielding will be designed as a two-piece system on a trolley that can be pulled away to allow access to the dilution unit for experiment installation (Fig. 1.6). Unfortunately, no shield can be put over the fridge due to some instrumentation fixed on top of it which is required for its operation.

To reduce the background coming from above a cylindrical metal shielding will be inserted in the fridge. Its thickness should be as small as possible as to reduce the cooling time of the fridge. Furthermore, although

[7] Which is directly proportional to the ionization energy.

[8] This machine, which produces neutrons through the reaction d + d $\rightarrow^3$ He + n accelerating deuteron ions on a deuteron target is very compact and portable (can be hand-carried by a strong person) and can be operated also in pulse mode.

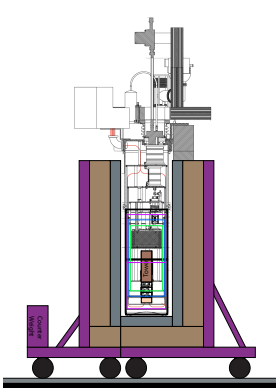

(a) Configuration with the closed shielding (the supports of the fridge are not drawn for the sake of clarity).

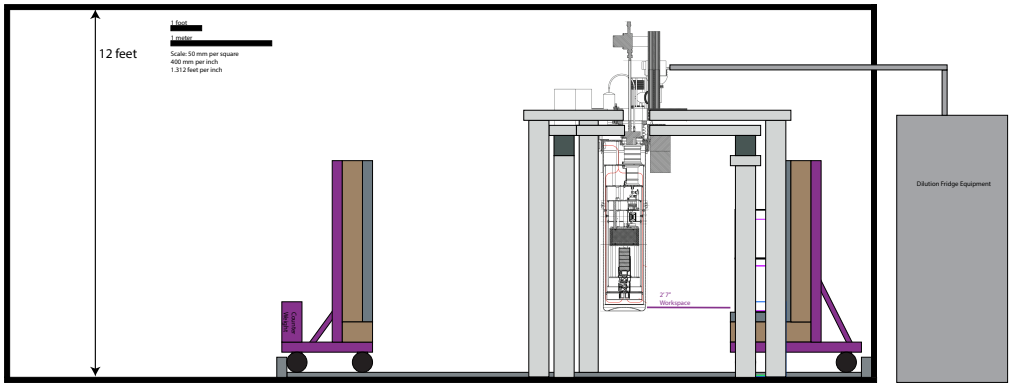

(b) Configuration with the shielding opened. The rails of the trolley and the supports of the fridge are well evident inside the clean room black rectangle. The box outside the clean room is the dilution fridge equipment.

Figure 1.6: Side view of a section of NEXUS@FNAL fridge and shielding. The lead shielding is drawn in grey, the plastic neutron moderator in brown.

lead is the best available shielding material from gamma rays, it would desirable to use copper instead owing to its far better heat conductivity at low temperatures.[9]

A sketch of the NEXUS@FNAL fridge is drawn in figure 1.7. The fridge is made up of an outer stainless steel can with three intermediate aluminium cans and an innermost copper can. The cylindrical inner copper shielding is well visible between the last can and the detector tower (the six iZIPs that are contained in the tower are drawn in red). The 10 cm lead outer shielding is drawn in blue and the 20 cm plastic neutron moderator in green. To get an idea of the dimensions of the apparatus, the height of the plastic neutron moderator is about 180 cm and its side length about 110 cm.

1.5 Aim of this study

The aim of the present study is to measure the background on-site at NEXUS@FNAL facility, to create the instruments to estimate the final background rate for an iZIP detector put into the fridge at and to check that it will be lower that the target value of 100 dru (events/keV/kg/day).[10] To accomplish this task, it was necessary to determine what are the minimum thickness and the best material for the inner shielding which allow to lower the background coming from above at the same level of that coming from the walls and from the bottom of the fridge while keeping at the same time the cooling time of the fridge as short as possible.

The report is organized in the following way: in the second chapter are described the calibration of the scintillator detectors used to measure the gamma background in the NuMI tunnel and the spectrum obtained in the actual measurements, whereas in the third chapter is described the *Geant4* [17] simulation that was developed to estimate the amount of gammas which will pass through the shielding as a function of the material and the thickness of the inner shielding. Finally, the order of magnitude of the background rate in the iZIP detectors is estimated.

[9] Lead gets superconductive under 7 K whereas copper is not a superconductor.

[10] This value was estimated considering a typical underground radioactivity level and a 4π shielding of 10 cm of lead.

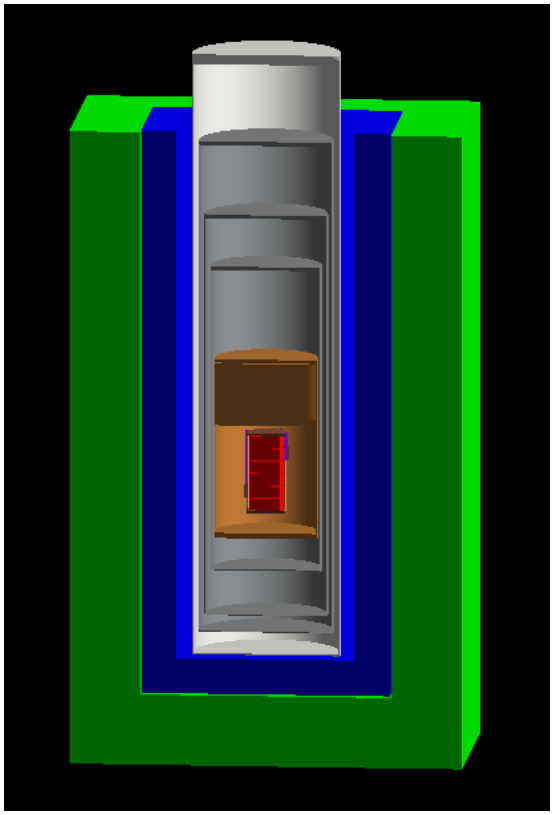

Figure 1.7: Section of the *Geant4* model of NEXUS@FNAL fridge developed for this project (for further details see chapter 3).

Chapter 2

Measurement of the gamma background at NuMI tunnel

In this chapter we describe the measurement of the gamma background at the NuMI tunnel. In the first sections, we describe the scintillator detectors that were used to perform the measurement and their calibration through some well known radioactive sources. Then, in the last section of the chapter, we present the spectra of the background that were acquired in the measurement in the tunnel.

2.1 Experimental apparatus

Two scintillator detectors were used to perform the measurement of the background in the NuMI tunnel: a *Victoreen 490 Thyac* NaI detector (cylindrical active volume of diameter 3.6 ± 0.2 cm and height 2.5 ± 0.5 cm), and a *Eljen 301* liquid scintillator detector (cylindrical active volume with both diameter and height equal to 5.0 ± 0.1 cm). They were powered by two *FLUKE 408B* high-stability high voltage supplies at 900 ± 1 V and -1460 ± 1 V respectively. A *RC* deriver was used to read the output of the NaI detector whose supply cable was used also for the data acquisition (DAQ). The case of the deriver was additionally grounded with a grounding cable to avoid a strong monochromatic noise whose source was not well understood. The output signal of the two detectors was sent to a *Caen DT5720* four-channels analog to digital converter (ADC) whose output was read by the computer via *daqman* DAQ software developed by Ben Loer [18]. Channel 1 of the ADC was used to acquire data from the EJ-301 detector and channel 2 from the NaI detector.

The whole experimental apparatus was mounted on a cart to make its transport to the NuMI tunnel easier (Fig 2.1). The calibration of the detectors and the data taking are described in detail in the next sections.

2.2 Calibration of the scintillator detectors

2.2.1 Workpoint and quality check

Attention was paid to always let the PMTs thermalise for about one hour before acquiring data. The ADC was set to sample the input voltages every 16 ns. It records signals up to 2 V_{pp} with 12 bit resolution. An offset voltage was introduced in the input signals in order to set the baseline voltage to ADC counts 3895. The trigger threshold was set to ADC counts 3875 for the NaI detector and to 3885 for the EJ-301 detector, just over the voltage value at which the electrical noise became dominant. Every time that the trigger is fired by one of the two detectors, data from 0.5 μs before the trigger time to 2.0 μs after the trigger time are recorded for both channels. The time window duration was chosen in order to record the whole NaI pulse, which lasted ~ 1 μs (the EJ-301 pulses are usually shorter than 200 ns).

The *daqman* DAQ software looks for pulses with well defined rising and falling edges within the time window defined by the trigger. Before analizing the data, a further quality check is performed requiring that the variables defined by *daqman* for the time window satisfy all the following conditions (see [18] for reference about the definition of the variables):

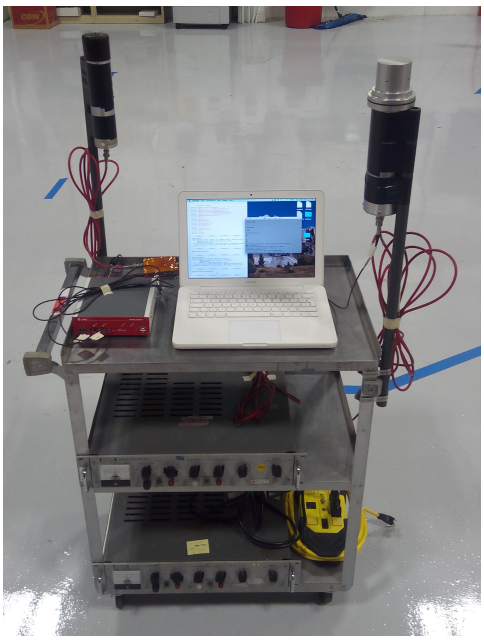

Figure 2.1: Experimental apparatus employed to perform the measurement of the gamma background. The two scintillators (NaI on the left, EJ-301 on the right) were kept about 50 cm over the surface of the cart to minimize the signals coming from backscattering gamma rays; the orange box behind the computer is the *RC* deriver used to read the NaI detector output.

- found_peak == 1 && peak_saturated == 0 guarantees that the research algorithm was successful and that the signal never saturated the ADC (anyway, this last condition was never verified);
- found_start == 1 && found_end == 1 to reject events which are not completely contained in the time window set by the trigger in order not to bias the measurement of the energy of the pulses (this happened very often while taking data with intense radioactive sources, when more than one pulse was present in the same time window). Anyway, these variables were not very efficient;
- start_time > -0.4 µs && start_time $< 1.$ µs assures that the previous condition is fulfilled by a different approach (in particular, a peak of events with start_ time $\simeq -0.5$ µs was observed before this condition was required);

The energy of every pulse was estimated through the pulses[0].integral variable, which sums the value of all the bins between the start and the end of the pulse after subtracting the baseline value.

2.2.2 Energy calibration

The energy calibration was performed acquiring the spectra of the radioactive source which are listed in Tab 2.1. Only the photopeaks and the Compton edges that were clearly recognizable were used as references. An example of the spectra is plotted in Fig. 2.2. The photopeaks are present in the NaI data but are not evident in the the EJ-301 data because the liquid scintillator is composed of elements whose atomic number is lower than that of the NaI elements (the photoelectric cross section scales as a power of the atomic number) and its density is lower than NaI density, so that multiple interactions are less likely.

The energy of the gamma line associated with the photopeak was assumed to be the one that corresponded to the maximum population within the photopeak;[1] the error was estimated as the half width at half maximum of the photopeak. The width of the photopeak is essentially a measure of the detector resolution. Since it is much larger than the typical energy scale within which the Compton spectrum changes, the relative maxima that are observed in the spectrum are at a slightly lower energy than the actual Compton edge. Following the estimations made in [19] the Compton edge energy was estimated as the energy (on the right

[1] This assumption implies that the energy resolution of the PMT is symmetric and that the energy spectrum around the photopeak is negligible with respect to it.

Table 2.1: Gamma lines and Compton edges employed to perform the energy calibration of the scintillation detectors.

Source	E (keV)	Type
^{133}Ba	207	Compton edge
^{22}Na	340	Compton edge
^{133}Ba	356	photopeak
^{137}Cs	478	Compton edge
^{22}Na	511	photopeak
^{137}Cs	662	photopeak
^{22}Na	1062	Compton edge
^{60}Co	1118	Compton edge
^{60}Co	1173	photopeak
^{22}Na	1275	photopeak
^{60}Co	1333	photopeak

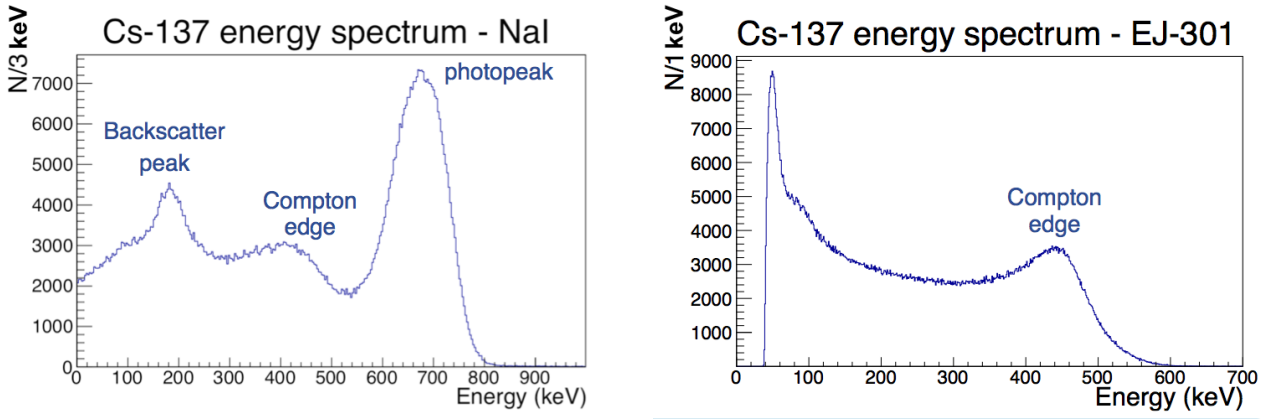

(a) NaI detector.

(b) EJ-301 detector.

Figure 2.2: ^{137}Cs spectrum acquired with the two scintillator detectors.

of the relative maximum) at which the distribution value is 80% of the relative maximum; the error was estimated as the semidispersion of the estimated Compton edge and the relative maximum. This approach probably introduces a little bias in the calibration; however, it is estimated to be negligible as far as our needs - recognizing the gamma lines of the background in the NuMI tunnel - are concerned.

The results of the calibration were fitted with a linear function and are plotted in Fig. 2.3. The energy scale is linear for both the detectors, but with very different conversion scale and offsets.

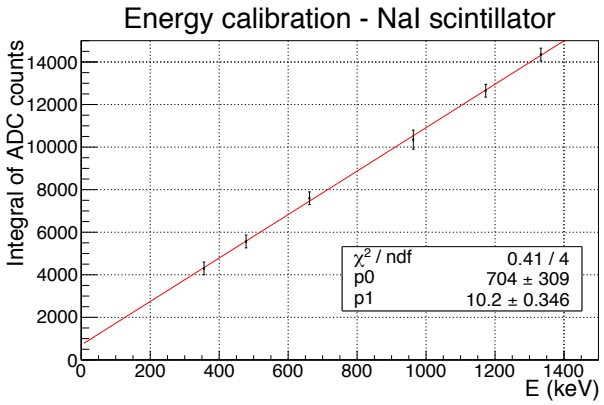

(a) NaI detector (both photopeaks and Compton edges are used). ^{22}Na source was the most intense and is not used because of some technical problems with the DAQ.

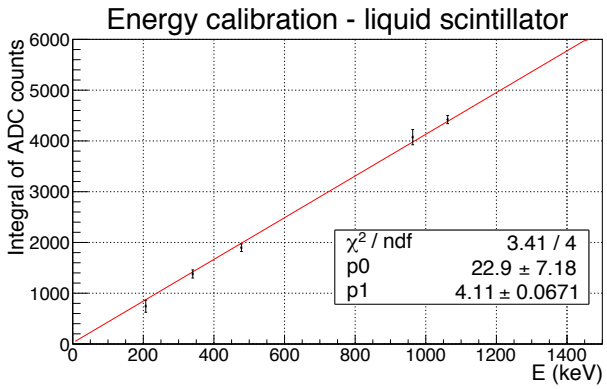

(b) EJ-301 detector (only the Compton edges are used).

Figure 2.3: Energy calibration of the scintillator detectors.

2.2.3 Efficiency measurement

The efficiency of the detection of the gamma rays was measured counting the rate of recorded pulses with a radioactive source at fixed distance from the detectors. The expected rate at which the gamma rays hit the detectors is just the activity of the source corrected by the mean number of gamma rays produced in one decay (Tab. 2.2), times the geometrical acceptance of the detector with respect to the source. The geometrical acceptance was calculated as the ratio between the area of the basis of the cylinder of scintillator which faced the source and the area of the sphere whose radius was equal to the distance between the source and the basis.[2] The ratio of the measured rate to the expected rate gives the efficiency of the detector. The measured rate was calculated after the DAQ program recognition of the peaks and the quality cuts, so that the so calculated efficiency is the convolution of the hardware detector efficiency and of the efficiency of the peak recognition of the DAQ program.

A preliminary run without source was performed to measure the rate of the environmental background; the result was subtracted from all the subsequent measurements. The distance of the source from the detector was varied from run to run in order to keep the measured rate well higher than the background one, but not as high as to cause the presence of significant dead time. The results are shown in Tab. 2.2.

Table 2.2: Measured efficiency for various radioactive sources. E is the energy of the highest photopeak of the source.

Source	E (keV)	ϵ_{NaI}	$\sigma_{\epsilon_{NaI}}$	ϵ_{EJ-301}	$\sigma_{\epsilon_{EJ-301}}$
^{133}Ba	356	0.34	0.04	0.18	0.02
^{137}Cs	662	0.30	0.03	0.14	0.01
^{22}Na	1275	0.45	0.04	0.21	0.02

The three measurements are not compatible nor there is a clear dependence of the efficiency on the energy. There was not enough time to further investigate this behaviour, nor other sources that could be

[2]The sources had a diameter smaller than 2.5 cm and were always placed at more than 15 cm from the detector, so a point-like model of the source is a good approximation for our aims.

used to enlarge the data set (^{60}Co was too weak with respect to the background). However, to the extent of the current measurement we are just interested in a rough estimation of the efficiency. Therefore, only the mean value of the measurements was considered supposing that the efficiency is independent of the energy and the uncertainty was conservatively estimated as the maximum difference between the measurements and the mean: $\epsilon_{NaI} = 0.35 \pm 0.10$ and $\epsilon_{EJ-301} = 0.16 \pm 0.05$.

2.3 Background measurement at the NuMI tunnel and the results

The data acquisition in the NuMI tunnel, taken at about three meters from the tunnel wall and three meters from the DAMIC clean room in the direction of MINOS experimental cavern,[3] lasted 13.6 hours. The obtained spectra are plotted in Fig. 2.4. Owing to the poor energy resolution, only the 1.461 MeV line of ^{40}K (Compton edge at 1.244 MeV) and the 2.614 MeV line from the ^{232}Th decay chain (Compton edge at 2.381 MeV) are clearly recognizable.

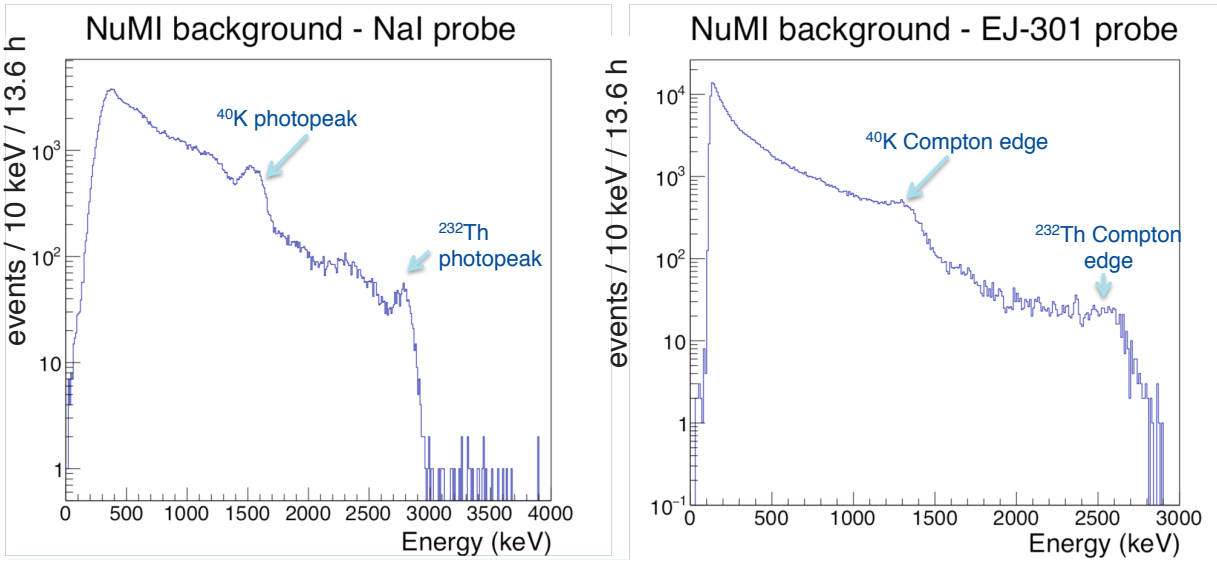

Figure 2.4: Spectra acquired in the NuMI tunnel in a 13.6 hours DAQ.

There is clearly an error in the energy calibration, likely due to the low energy spectrum of the sources that were used to perform the calibration. In fact, the linear function that was used to fit the reference points of the calibration sources was extrapolated to higher energies to determine the energy scale of the spectra in Fig. 2.4. Anyway, the energy of the highest photopeak used for the calibration was 1333 keV whereas the ^{232}Th photopeak is at 2614 keV, which is nearly the double of the first. This means that every error present in the calibration at 1333 keV might be doubled at the ^{232}Th photopeak. Furthermore, there might be non-linear effects in the DAQ that become not negligible only at high energies.[4] The origin of wrong energy scale is still under investigation. In the future development of the design studies for NEXUS@FNAL facility it would be desirable to use also the ^{40}K and ^{232}Th photopeaks to perform the calibration. The aim of the present study is not, however, invalidated by the imperfect energy calibration and no further effort was made to improve it.

[3] The fridge will be probably set up in this place.

[4] One of these effects might be a bad setting of the baseline value by the DAQ program.

Chapter 3

NEXUS@FNAL simulation in *Geant4*

3.1 *SuperSIM* model

SuperSIM is the *Geant4* [17] simulation framework developed to run all the simulations required by the SuperCDMS collaboration. So far, it was completely developed by Michael Kelsey (SLAC). Its libraries describe the experimental sites, cryogenic apparata and SuperCDMS detectors in great detail. However, the cryogenic fridge and the shielding that will be bought to be installed in the NEXUS@FNAL facility are not described in *SuperSIM* standard release. The main goal of the present project was to develop a *Geant4* simulation of the fridge and of the shielding (both the internal metal cylindrical one and the external lead and plastic moderator one) of NEXUS@FNAL to estimate their rejection power of gamma and neutron radiogenic background.[1]

The model drawn in Fig. 1.7 was developed from scratch (with the exception of the iZIPs detectors), and a user interface was implemented to run the simulations from a standard *Geant4* macro. Through this interface the user is allowed to run simulations with or without the inner and/or outer shielding and to change the material and the thickness of the internal shielding.[2] The complete documentation with the detailed dimensions of the fridge and of the shielding and the commands for the user interface can be found in appendix A. The instructions to add a new detector geometry to *SuperSIM* are described in appendix B.[3]

3.2 Simulations: first results

There was not enough time to perform the full set of the required simulations. Since no information about the space distribution of the gamma rays was available, it was decided to assume an isotropic distribution simulating a contamination of an unstable radioactive isotope on a sphere with 2.5 m radius and centred in the SuperCDMS tower of detectors. The radius was chosen to contain the whole fridge and shielding; only simulations with ^{238}U contamination where performed because little time was available and this isotope turned out to be the one whose decay chain was simulated most quickly among the isotopes that are expected to form most of the background (^{40}K, ^{232}Th and ^{238}U).

Four different configurations were taken into account:

- without shielding, used as a reference to correct for the fact that the geometrical acceptance of the detectors for the simulated decays is clearly less than one;
- with outer shielding and 25 mm of lead inner shielding;
- with outer shielding and 25 mm of copper inner shielding to compare the stopping power of copper with the lead's one;

[1] The rejection power is defined as the reciprocal of the fraction of background particles which pass through the shielding and hit the detector.

[2] The outer lead shielding will be made up of bricks of 5 cm x 10 cm x 20 cm and it won't be possible to increase its thickness within the project budget.

[3] This was the first attempt to add a new facility geometry to *SuperSIM* by a person different from Michael Kelsey. As the procedure described in the available documentation is not complete, it might be useful to present a complete one for who would like to add another geometry to *SuperSIM* in the future.

- with outer shielding and 175 mm of copper inner shielding (175 mm is the maximum thickness that can be used for the inner shielding).

The obtained spectra for the events that deposit energy in one and only one of the iZIP detectors are shown in Fig. 3.1.[4] The number of simulated events was increased as the thickness of the inner shielding increased to keep the statistical errors under control (it is, however, evident that more simulations are required to obtain a reliable spectrum over 1.5 MeV); the obtained spectra are normalized to the number of events that were simulated in the case without shielding to allow a direct comparison of the simulations. Two further simulations with 50 mm of copper and 75 mm of copper inner shielding (plus the outer shielding) were performed, but they are not shown in Fig. 3.1 for sake of clarity.

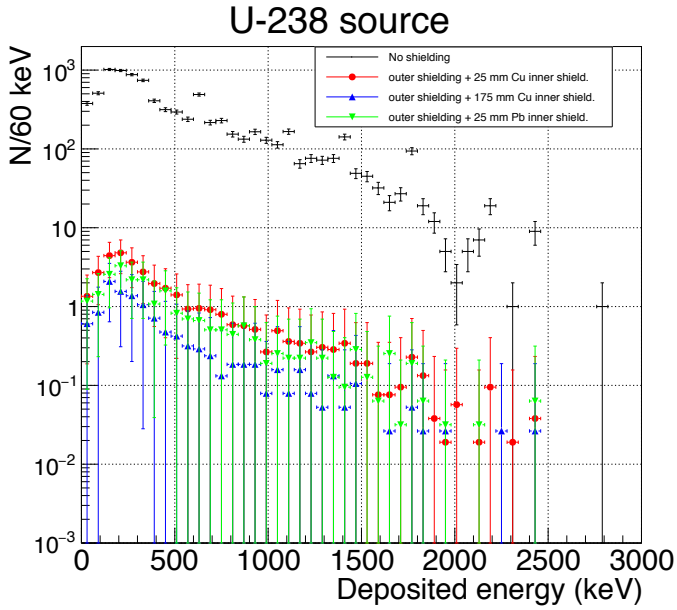

Figure 3.1: *SuperSIM* simulation of a ^{238}U isotropic contamination from the outer environment for different combinations of material and thickness of the inner shielding (the outer shielding is always present when the inner shielding is present). The simulation without both the components of the shielding is reported in black for reference; some of the gamma lines of the ^{238}U decay chain are well evident. The simulation is not reliable over about $1.5 \sim 2$ MeV due to low statistics.

A rejection power of ~ 200 is obtained already with 25 mm of copper inner shielding and the outer shielding with respect to the simulation without shielding.[5] The improvement obtained with the same thickness of lead gives an improvement of less than a factor two; this result is in good agreement with the previsions that can be done looking at the attenuation lengths plotted in Fig. 3.2 in the range 300 keV $\sim$ 3 MeV. Therefore, it is likely that the use of lead instead of copper will not be strictly necessary for NEXUS@FNAL.

However, the increase of the rejection power, for example for 1 MeV gamma rays, is lower than expected. In fact, from Fig. 3.2 we can estimate the attenuation length in copper at this energy in about $2 \sim 3$ cm (copper has a density of about 8.9 g/cm^3). Supposing that all the background is due to the gamma rays coming from the top, the rejection power should increase of about $(0.1 \sim 1.8) \cdot 10^3$ when the thickness of the inner shielding grows from 2.5 cm to 17.5 cm, while the observed increase is only about a factor of four.

This fact is probably due to the mechanism displayed in Fig. 3.3a: some photons coming from the top of the fridge propagate around the shielding, scatter on the walls of the cans and finally hit the detectors. As a first check of this hypothesis the $\cos\theta$ distribution of the points on the sphere where the decays were simulated was plotted for the events in which the gamma rays eventually hit one and only one detector (Fig. 3.3b). The result confirms that more than half of the events come from the top of the fridge ($\cos\theta > 0.85$). An easy estimate shows that only particles with $\cos\theta \gtrsim 0.97$ can hit the fridge without passing through the outer

[4] The standard trigger used by SuperCDMS collaboration for the detector tower to reduce the background requires this condition.

[5] From this point forward the outer shielding is always assumed.

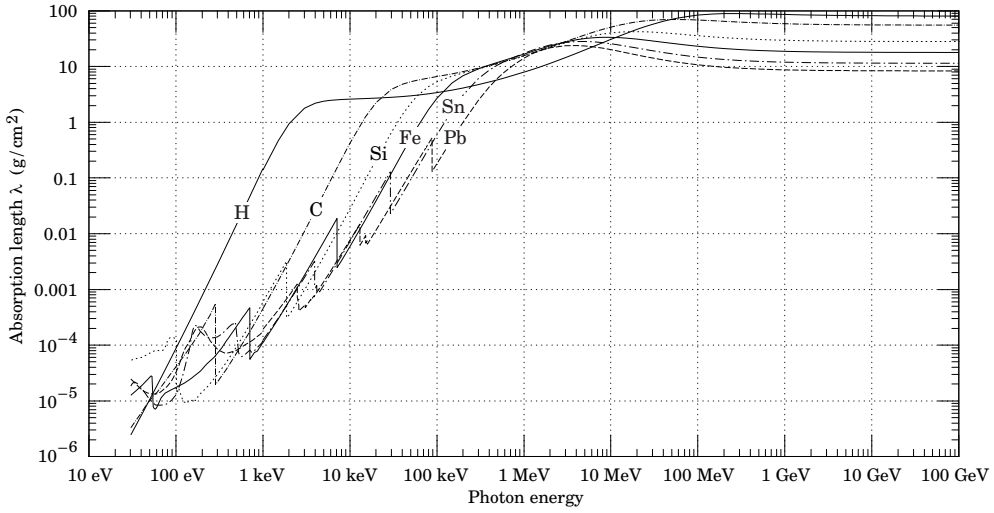

Figure 3.2: Attenuation length of photons for different materials; figure taken from [20].

lead shielding. This value coincides with the FWHM of the $\cos\theta$ distribution and supports the hypothesis of a dominant background from scattering of photons in the fridge. Further studies are going to be performed to examine the most probable paths through the shielding for the photons.

3.3 Estimate of the background rate with 175 mm of copper inner shielding

Taking advantage of the preliminary results of the background measurement in the NuMI tunnel and of the *SuperSIM* simulation, it was possible to estimate the order of magnitude of the expected background rate for a SuperCDMS detector tested in the NEXUS@FNAL facility in presence of the outer shielding and 175 mm of copper inner shielding.

A rejection power of about 500 can be conservatively estimated from Fig. 3.1 over the whole gamma energy spectrum. Moreover, the gamma lines which are present in the unshielded configuration disappear in the shielded one. Considering for example the NaI probe, the mass of the scintillating detector is about 0.09 kg and the detection efficiency is about 0.35, whereas the background run lasted about 13.6 hours. The background rate can than be estimated, in first approximation, looking at the population of the bins in Fig. 2.4. The bin population goes from about 2000 at 500 keV to about 200 at 2 MeV (and further decreases as the energy increases) and the bins width is 10 keV. So the background rate at is roughly:

$$\frac{1}{0.35}\cdot\frac{2000}{10\ \text{keV}\cdot 13.6\ \text{h}\cdot 0.09\ \text{kg}}\cdot\frac{1}{500}=22\ \text{dru}$$

at 2 MeV, whereas the background at 500 keV is expected to be an order of magnitude over this value.

This estimate is close to the final goal of a background rate less than 100 dru. This fact is very encouraging both because the estimate of the rejection ratio was quite optimistic and the background might be easily further reduced if its main source is the scattering among the cans of photons coming from the top. In fact, in this case it would suffice to put some lead bricks on the top of the fridge - wherever the tubes and the top instrumentation will allow it - to block part of the line of sight of the photons around the inner shielding and to reduce considerably the number of photons which hit the detector. This hypothesis will be examined in the next months.

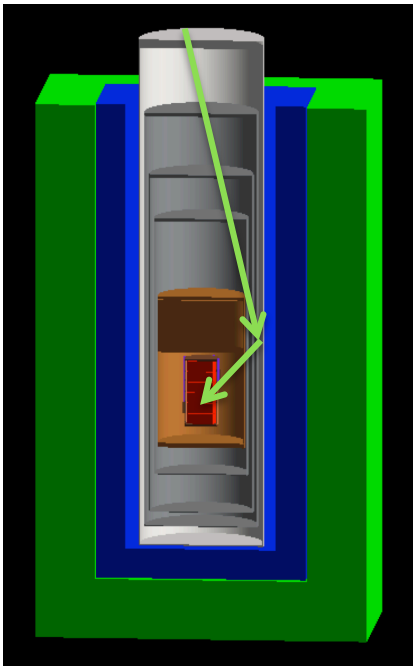

(a) Gamma rays possible path around the shielding.

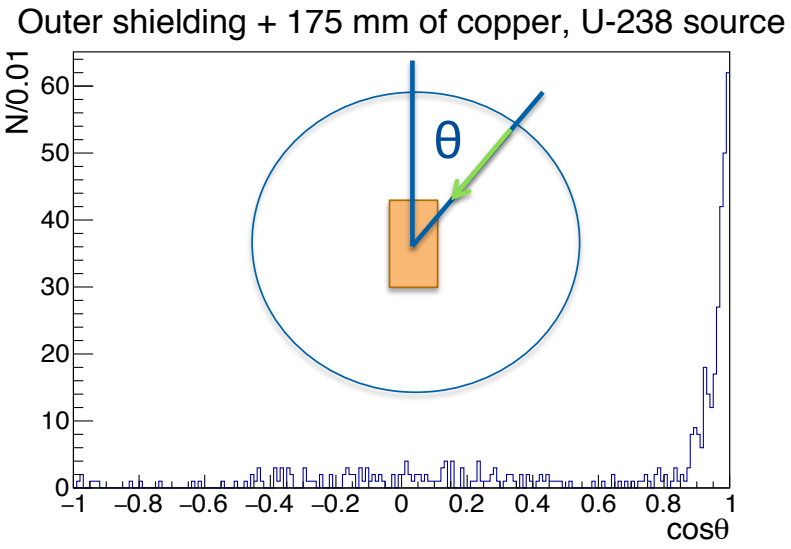

(b) Angular distribution of the ^{238}U decays on the sphere where the atoms were generated by the simulation for the events for which the photons eventually hit one and only one detector. For sake of clarity the coordinate system is represented in a drawing where the detector is schematised as a yellow rectangle.

Figure 3.3: Probable main source of background for the facility configuration with the outer shielding and 175 mm of copper inner shielding.

Future perspectives

NEXUS@FNAL will be a new low background testing facility for high precision cryogenic detectors at NuMI tunnel at Fermilab. In the present work a first measurement of the background was performed in the NuMI tunnel and a simulation of the facility was prepared in *Geant4* and integrated into *SuperSIM* to perform the design studies needed to determine the thickness of the shielding from radiogenic gamma background. A first encouraging estimate of the background rate measured by the detectors that will be tested has been made, but more studies are required to improve the precision of this result.

First of all, a new longer measurement of the background in the NuMI tunnel is desirable to identify the less populated photopeaks in the spectrum. Then, a *Geant4* simulation of the scintillator detectors should be developed and a linear combination of the spectra obtained simulating ^{40}K, ^{232}Th and ^{238}U decays measured by them should be used to fit the measured spectrum. This simulation would fix, together with the measurement of the background in the NuMI tunnel, the normalization of the simulations that were described in chapter 3 so that they would become directly comparable with the rate that will be measured by SuperCDMS detectors. The estimate of the expected background made following this approach would be much more reliable than the present one.

Secondly, new simulations should be performed with intermediate thickness of copper (e.g. 125 mm) for the internal shielding, to verify if 175 mm of copper are really needed to keep the background low or if the background is already saturated by the scattering photons from the top already at medium thickness. A reduction of the thickness of copper would lower the cooling time and make the operation of the fridge quicker. Finally, new simulations performed adding some lead bricks on top of the fridge could be used to confirm the hypothesis that the scattering photons are the main source of background and to estimate the final background rate in the detector after this further shielding will be set up.

Appendix A

SuperSIM documentation for NEXUS@FNAL facility

A.1 User interface commands to perform simulations at the NEXUS@FNAL facility

/CDMS/Detector NEXUS

- use the NEXUS@FNAL experimental setup
- dry dilution fridge with 5 cans, one SuperCDMS tower and optional outer and inner shieldings

/CDMS/NEXUS/verbose n

- n = 0 (default): no output
- n = 1: basic output
- n = 2: detailed output

/CDMS/NEXUS/Shielding int

- int = 1 builds the outer shielding (10 cm lead + 20 cm plastic on the walls and on the bottom), int = 0 does not
- command default: 1
- constructor defalut: 1

/CDMS/NEXUS/InnerShielding int

- int = 1 builds the inner shielding (a cylinder of metal over the SuperCDMS tower), int = 0 does not
- command default: 1
- constructor defalut: 1

/CDMS/NEXUS/InnShieldMat string

- sets the material of the inner shielding
- possible candidates: copper, lead
- command default: copper
- constructor default: copper

/CDMS/NEXUS/InnShieldThick_in_mm double

- sets the thickness of the inner shielding
- possible candidates: between 0 and 176
- command default: 75
- constructor default: 75

A.2 Geometrical description

The whole geometry and dimensions of *SuperSIM* simulation of NEXUS@FNAL are set in supersim/CDMSgeometry/detectors/NEXUS.cc. The documentation which describes the members of the objects that are used to store the geometrical dimensions of the various cans and of the elements of the shielding can be found in supersim/CDMSgeometry/detectors/NEXUS.hh. If a sixth can will be present in the fridge - this might be the case for some models -, it can be easily added just pushing back a new CanData object to the fCans vector. The physical dimensions of the cans and of the outer shielding are described in Tab. A.1 and in Tab. A.2. The inner shielding is a metal cylinder of 292 mm diameter which starts exactly at the lower surface of the cap of the innermost can and develops from the top down.

Table A.1: Physical volumes of the *SuperSIM* simulation of the fridge. The fridge is schematised with five cans; the thickness (th.) of the upper caps is doubled with respect to the actual one to take into account the further components (metal tubes, flanges, etc.) which will be present on their top. The vertical shift is the coordinate of the centre of the cylinders in the frame of reference centred in the centre of the SuperCDMS tower inserted in the fridge.

Name	Height (mm)	Inner diameter (mm)	Walls th. (mm)	Upper cap th. (mm)	Lower cap th. (mm)	Vertical shift (mm)	Material
Can_0	1708.2	414	4.0	28	4.0	517.7	stainless steel
Can_1	1396.2	378	1.5	12	2.0	452.7	aluminium
Can_2	1139.3	346	1.0	10	1.5	405.0	aluminium
Can_3	864.2	313	1.0	10	3.5	277.0	aluminium
Can_4	509.0	292	1.0	10	15.0	185.7	copper

Table A.2: Physical volumes of the *SuperSIM* simulation of the bucket-shaped outer shielding. The vertical shift is the absolute value of the z coordinate of the upper surface of the base in the frame of reference centred in the centre of the SuperCDMS tower inserted in the fridge.

Name	Inner side (mm)	Height (mm)	Walls th. (mm)	Base th. (mm)	Vertical shift (mm)	Material
Shield_0	700	1800	200	200	634	polyethylene
Shield_1	500	1600	100	100	529	lead

Appendix B

SuperSIM additional documentation: adding a new geometry to *SuperSIM*

As the procedure to add a new geometry to *SuperSIM* is not trivial and the currently available documentation skips some details of the procedure, the needed instructions to add a detector geometry to *SuperSIM* are itemized in the following (the line number reference corresponds to the 7.2 release of *SuperSIM*):

1. The header and source files which describe the detector geometry, <detectorName>.hh and <detectorName>.cc, should be saved in supersim/CDMSgeometry/detectors/. They should implement at least the following functions:
   - the constructor of the detector <detectorName>. It should be declared as a derived class of CDMSDetectorBase with public access specifier and determines the default values of the parameters of the detector;
   - virtual G4LogicalVolume* BuildGeometry() - builds all the physical volumes of the apparatus and returns the pointer to the world physical volume;
   - virtual G4double GetRadius() const - returns the largest radial dimension of the apparatus;
   - virtual G4double GetLength() const - returns the largest z dimension of the apparatus;
   - all sensitive detectors should call the DependsOn() function to record their interactions with particles in the output files.
2. The files which implement the user interface, <detectorName>Messenger.hh and <detectorName>Messenger.cc, should be saved in supersim/CDMSgeometry/interface/.
3. Add the following lines to supersim/CDMSgeometry/interface/CDMSGeometryManager.hh:
   - #include "CDMSgeometry/detectors/<detectorName>.hh"
     (line 114);
   - SelectDetCmd->SetGuidance(" <detectorName> : <detector description>");
     (line 222);
   - add "<detectorName>"
     to the possible candidates in the command SelectDetCmd->SetCandidates("..."); (line 223)
   - if (name == "<detectorNameLowercase>") theDet = geomManager->Get<detectorName>();
     (line 402); <detectorNameLowercase> is <detectorName> with all the letters converted to lowercase.
4. Add the following lines to supersim/CDMSgeometry/interface/CDMSGeomMessenger.cc:
   - class <detectorName>;
     to the class declarations (line 106);

- <detectorName>* Get<detectorName>();
  to the list of the public functions (line 142);
- <detectorName>* the<detectorName>;
  to the list of the private member pointers to the detectors objects (line 212).

5. Add the following lines to supersim/CDMSgeometry/interface/CDMSGeometryManager.cc:

   - #include "CDMSgeometry/detectors/NEXUS.hh"
     (line 84);
   - the<detectorName>(0)
     to be added to the CDMSGeometryManager::CDMSGeometryManager() constructor (in line 110);
   - delete theNEXUS; theNEXUS=0;
     to the destructor (line 141);
   - if (theNEXUS) theNEXUS->CheckGeometry(checkGeom);
     to CDMSGeometryManager::CheckGeometry function body (line 192);
   - NEXUS* CDMSGeometryManager::GetNEXUS() {
     if (!theNEXUS) theNEXUS = new NEXUS;
     return theNEXUS;
     }
     to the "Complete detector assemblies with various configurations" list (lines 264-267).

Obviously, every time that a file is modified in supersim directory, *SuperSIM* should be recompiled prompting the make all command from within the supersim directory.

Bibliography

1. Einasto, J. Dark Matter. *ArXiv e-prints.* arXiv: 0901.0632 [astro-ph.CO] (Jan. 2009).
2. Ade, P. A. R. *et al.* Planck 2015 results. XIII. Cosmological parameters. *Astron. Astrophys.* **594,** A13 (2016).
3. Silk, J. *et al. Particle Dark Matter: Observations, Models and Searches* (ed Bertone, G.) (Cambridge University Press, 2010).
4. Goodman, M. W. & Witten, E. Detectability of certain dark-matter candidates. *Phys. Rev. D* **31,** 3059–3063 (12 June 1985).
5. Cerdeno, D. G. & Green, A. M. Direct detection of WIMPs. arXiv: 1002.1912 [astro-ph.CO] (2010).
6. Agnese, R. *et al.* Search for Low-Mass Weakly Interacting Massive Particles with SuperCDMS. *Phys. Rev. Lett.* **112,** 241302 (24 June 2014).
7. Ahmed, Z. *et al.* Dark Matter Search Results from the CDMS II Experiment. *Science* **327,** 1619–1621. ISSN: 0036-8075 (2010).
8. Akerib, D. S. *et al.* First results from the cryogenic dark matter search in the Soudan Underground Lab. *Phys. Rev. Lett.* **93,** 211301 (2004).
9. Wang, G. Phonon emission in germanium and silicon by electrons and holes in applied electric field at low temperature. *J. Appl. Phys.* **107** (2010).
10. Agnese, R. *et al.* New Results from the Search for Low-Mass Weakly Interacting Massive Particles with the CDMS Low Ionization Threshold Experiment. *Phys. Rev. Lett.* **116,** 071301 (7 Feb. 2016).
11. Agnese, R. *et al.* Projected Sensitivity of the SuperCDMS SNOLAB experiment. *Submitted to: Phys. Rev. D.* arXiv: 1610.00006 [physics.ins-det] (2016).
12. Yellin, S. Finding an upper limit in the presence of an unknown background. *Phys. Rev. D* **66,** 032005 (3 Aug. 2002).
13. Lindhard, J., Nielsen, V., Scharff, M. & Thomsen, P. *Integral Equations Governing Radiation Effects* (Munksgaard i komm, Copenaghen, 1963).
14. Chavarria, A. E. *et al.* Measurement of the ionization produced by sub-keV silicon nuclear recoils in a CCD dark matter detector. arXiv: 1608.00957 [astro-ph.IM] (2016).
15. Barker, D., Wei, W.-Z., Mei, D.-M. & Zhang, C. Ionization efficiency study for low energy nuclear recoils in germanium. *Astroparticle Physics* **48,** 8–15. ISSN: 0927-6505 (2013).
16. Chavarria, A. *Response of a CCD to low energy nuclear recoils from a 124Sb-9Be photo-neutron source* Presentation at the workshop Calibration of Low Energy Particle Detectors. Chicago, Sept. 24, 2015. <https://kicp-workshops.uchicago.edu/2015-lowecal/presentations.php>.
17. *Geant4 official site* <https://geant4.web.cern.ch/geant4/>.
18. Loer, B. *DAQMAN documentation* <https://github.com/bloer/daqman>.
19. Zhang, S.-Y.-L.-T. *et al.* Study on gamma response function of EJ301 organic liquid scintillator with GEANT4 and FLUKA. *Chin. Phys.* **C37,** 126003 (2013).
20. Olive, K. A. *et al.* Review of Particle Physics. *Chin. Phys.* **C38,** 090001 (2014).